

RESEARCH ARTICLE

10.1002/2016JG003754

Key Points:

- Significant amount of DOC export from surface soil by leaching
- Net retention of surface DOM leachates in deep soils
- Selective molecular exchange of soil DOM leachate during percolation

Supporting Information:

- Supporting Information S1

Correspondence to:

X. Zhang,
xz510@ufl.edu

Citation:

Zhang, X., J. A. Hutchings, T. S. Bianchi, Y. Liu, A. R. Arellano, and E. A. G. Schuur (2017), Importance of lateral flux and its percolation depth on organic carbon export in Arctic tundra soil: Implications from a soil leaching experiment, *J. Geophys. Res. Biogeosci.*, 122, 796–810, doi:10.1002/2016JG003754.




Received 22 DEC 2016

Accepted 16 MAR 2017

Accepted article online 22 MAR 2017

Published online 11 APR 2017

Importance of lateral flux and its percolation depth on organic carbon export in Arctic tundra soil: Implications from a soil leaching experiment

Xiaowen Zhang¹ , Jack A. Hutchings¹ , Thomas S. Bianchi¹ , Yina Liu², Ana R. Arellano¹, and Edward A. G. Schuur^{3,4}
¹Department of Geological Sciences, University of Florida, Gainesville, Florida, USA, ²Environmental Molecular Sciences Laboratory, Pacific Northwest National Laboratory, Richland, Washington, USA, ³Center for Ecosystem Science and Society and Department of Biological Sciences, Northern Arizona University, Flagstaff, Arizona, USA, ⁴Department of Biology, University of Florida, Gainesville, Florida, USA

Abstract Temperature rise in the Arctic is causing deepening of active layers and resulting in the mobilization of deep permafrost dissolved organic matter (DOM). However, the mechanisms of DOM mobilization from Arctic soils, especially upper soil horizons which are drained most frequently through a year, are poorly understood. Here we conducted a short-term leaching experiment on surface and deep organic active layer soils, from the Yukon River basin, to examine the effects of DOM transport on bulk and molecular characteristics. Our data showed a net release of DOM from surface soils equal to an average of 5% of soil carbon. Conversely, deep soils percolated with surface leachates retained up to 27% of bulk DOM while releasing fluorescent components (up to 107%), indicating selective release of aromatic components (e.g., lignin and tannin), while retaining nonchromophoric components, as supported by spectrofluorometric and ultrahigh-resolution mass spectroscopic techniques. Our findings highlight the importance of the lateral flux of DOM on ecosystem carbon balance as well as processing of DOM transport through organic active layer soils en route to rivers and streams. This work also suggests the potential role of leachate export as an important mechanism of C losses from Arctic soils, in comparison with the more traditional pathway from soil to atmosphere in a warming Arctic.

1. Introduction

Temperature in the Pan-Arctic region is predicted to increase 3–10°C by the end of this century [Intergovernmental Panel on Climate Change, 2013]. As a result, permafrost, or perennially frozen soil, in this region is vulnerable to enhanced thaw, leading to the potential microbial decomposition of permafrost organic carbon (OC). Permafrost soils have accumulated over hundreds to thousands of years and store half of global belowground organic carbon (~1700 Pg) [Tarnocai et al., 2009; Schuur et al., 2015], largely due to slow microbial decomposition in a cold environment [Hicks Pries et al., 2012; Vonk et al., 2013a]. Thawing of permafrost allows the release of previously frozen organic carbon (OC) into the contemporary carbon cycle by mobilization of dissolved and particulate OC (DOC and POC) as well as the release of greenhouse gases (CO₂ and CH₄) [Schuur et al., 2009; Rowland et al., 2010; Spencer et al., 2015].

As for the mobilization of permafrost OC, previous studies have focused on the transport of permafrost-derived DOC, because it is the major form of OC (80%) from Arctic river watersheds [Dittmar and Kattner, 2003]. The magnitude and composition of DOC/dissolved organic matter (DOM) exported from the Arctic soils varies with season, with the spring freshet exporting lignin-rich, young, and aromatic DOM while the late summer, when active layers are deepest, exports less bioavailable, less aromatic, older, and lower molecular weight DOM [e.g., Raymond et al., 2007; Striegl et al., 2007; Spencer et al., 2008]. However, the mechanisms behind this are still poorly understood, especially with active layer deepening—resulting in exposure of previously frozen soil to transport processes [Neff et al., 2006; Wickland et al., 2007; Frey and McClelland, 2009].

The fate and transport of DOM released from thawing soils will in part be controlled by molecular composition at different soil depth as well as hydrological flow paths (e.g., through surface versus deep soils) [Guo and Macdonald, 2006; Spencer et al., 2008; O'Donnell et al., 2014]. Conceptual models of vertical movement of DOM in soils has been well reviewed by Kaiser and Kalbitz [2012], summarizing the importance of physical, chemical, and biological effects. Ward and Cory [2015] showed the difference in chemical composition of

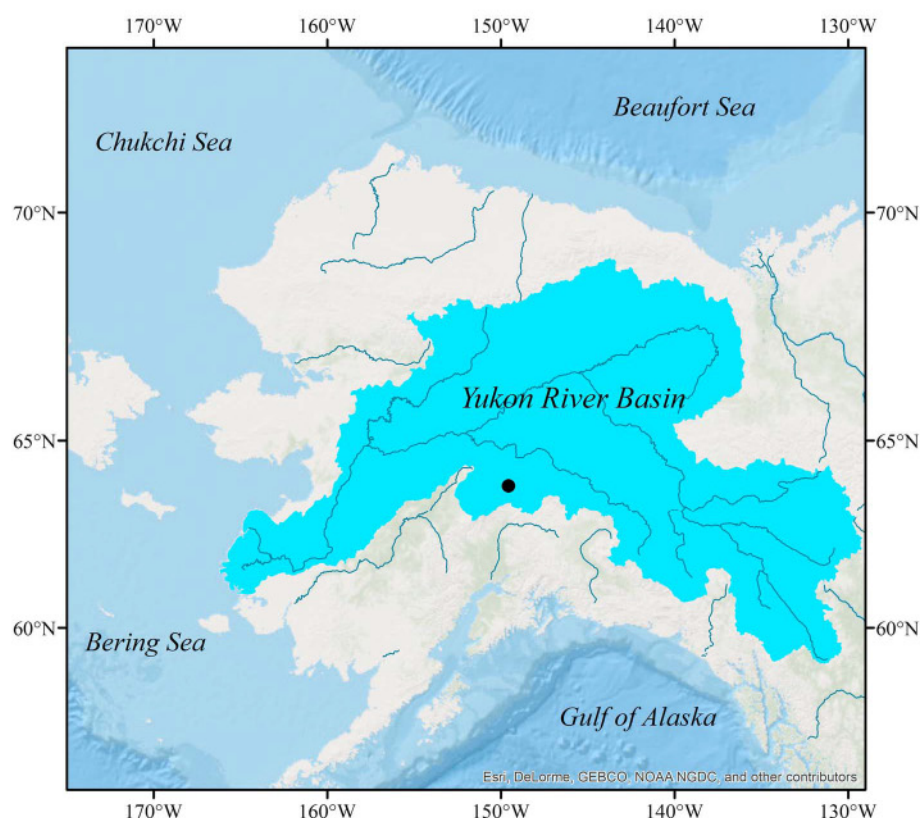


Figure 1. Map of the Yukon River basin and sampling location (black dot).

DOM from surface organic soils and deep mineral soils in the Arctic. However, these researches focused only on the differences between organic versus mineral soils. In permafrost regions, especially continuous permafrost, most surface runoff only percolates through the very top of soil (in the organic soil layer). Thus, there remain gaps in our knowledge on the role of export from leaching in overall C losses from Arctic soils, or, more specifically, what chemical changes occur in the formation of DOM leachate and how those changes are linked with the chemical composition of DOM in Arctic rivers [e.g., *Spencer et al.*, 2008; *Cao et al.*, 2016; *Mann et al.*, 2016]. Here we describe results from an Arctic soil leaching experiment, using soils collected from the Yukon River basin, to investigate DOM transformations during vertical infiltration through the organic soil layer as well as the importance of soil infiltration in the lateral transport of DOM.

In this study, we used a laboratory experiment to provide a proof-of-concept using state-of-the-art chemical techniques. Chemical changes in soil leachate DOM were investigated using Fourier transform ion cyclotron resonance mass spectrometry (FT-ICR-MS), chromophoric dissolved organic matter (CDOM), and fluorescent dissolved organic matter (FDOM), measured using excitation emission matrix (EEM) fluorescence. EEMs have been widely used to provide compositional information of DOM in a diversity of aquatic environments, including lakes, wetlands, and estuaries [Coble, 1996; Stedmon et al., 2003; Chen and Jaffé, 2014]. FT-ICR-MS, an ultrahigh-resolution mass spectrometric technique, has been applied more frequently in environmental sciences to provide an unprecedented means for understanding detailed molecular-level characteristics of DOM—which is commonly outside of the traditional analytical window [Kujawinski et al., 2002; Sleighter and Hatcher, 2007; Kellerman et al., 2015]. Extensive work on the chemical composition of DOM in the Yukon River [e.g., Guéguen et al., 2006; Striegl et al., 2007; Spencer et al., 2008; O'Donnell et al., 2014; Cao et al., 2016], as well as extensive soil incubation experiments [e.g., Mikan et al., 2002; Schuur et al., 2009; Sistla et al., 2013; Natali et al., 2014; Hicks Pries et al., 2015], makes the application of the lab leachate experiment particularly useful in examining soil-to-river versus soil-to-atmosphere linkages in C transport.

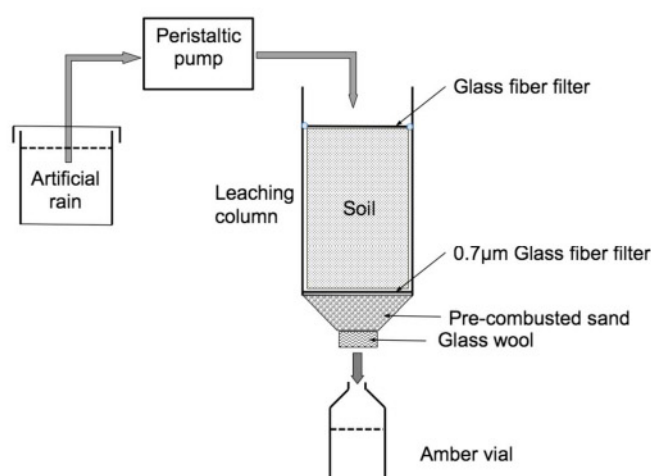


Figure 2. Leaching column design, as modified from Hodson and Langan [1999].

2014]. This region is characterized by moist acidic tundra—vegetated dominantly by tussock-forming sedge, graminoid, dwarf shrubs, and various mosses and lichens [Schuur *et al.*, 2009]. Soils were classified as Gelisol and are composed of 0.3–0.5 m thick organic horizon on top of cryoturbated mineral soil mixture of wind-blown loess and glacial till (small stones and cobbles) [Schuur *et al.*, 2009; Hicks Pries *et al.*, 2015]. Soil organic carbon pools with 1 m of the soil are $\sim 50 \text{ kg C/m}^2$, and the active layer thaws up to $\sim 60 \text{ cm}$ during growing season [Natali *et al.*, 2014]. Although located in a discontinuous permafrost region, this site is fully underlain by permafrost. Permafrost thaw features (e.g., thermokarst) have been documented over the past several decades in the nearby region [Osterkamp, 2007; Schuur *et al.*, 2009].

Soil samples were kept frozen and split lengthwise down the core in $\sim 5 \text{ cm}$ intervals in a -10°C cold room using band saw at the University of Alaska, Fairbanks. Samples were then shipped frozen to University of Florida and kept in a -80°C refrigerator before the experiment.

2.2. Laboratory Leaching Experiment

We conducted a three-stage laboratory leaching experiment to investigate DOC transformations during vertical percolation during short-term equilibration. Surface soil (S, 10–26 cm, two sample sections) and deep soil (D, 40–61 cm, two sample sections) from each core were used. Two lengthwise replicates from each core were used during leaching (Tables S1 and S2 in the supporting information). Surface soils (E1-S and E2-S) were sequentially leached with 220, 120, and 120 mL of artificial rain (Figure 2) during stages one, two, and three, respectively, and frozen overnight between stages to minimize microbial processing between days (Figure 3). Approximately half of surface soil leachates were percolated through the deep soils (E1-D and E2-D) using the same approach as above. Our initial leaching volume of 220 mL was based on our expectations from other soil leaching experiments to reach asymptotic DOC concentrations [Bohan *et al.*, 1997; Guo *et al.*, 2007]. The experiment was continued for two additional days (stages) until asymptotic concentrations were reached.

Soil samples were shaped to fit into a 60 mL syringe using a chisel while still frozen. Syringes were acid washed and tested for blank DOC and EEMs. Artificial rain was made with NH_4NO_3 , CaSO_4 , MgSO_4 , K_2SO_4 , and Na_2SO_4 dissolved in Milli-Q water and adjusted to $\text{pH} = 5.24$ with 6 N HCl to simulate natural precipitation in Denali National Park-Mount McKinley from National Atmospheric Deposition Program averaged for the last 35 years. Samples were thawed in a refrigerator at 4°C for 1 day to collect initial pore water. Then, surface soil samples were leached with artificial rain at a rate of $\sim 14 \text{ mL/h}$ at 20°C . As shown in Figure 2, the artificial precipitation was dripped at a constant rate onto soils using a peristaltic pump. Leachates were filtered by $0.7 \mu\text{m}$ Glass fiber filter and collected in 40 mL amber vials. Syringes were also wrapped in aluminum foil to minimize any possible photochemical reactions. Leachates were collected every 20 mL. Ten milliliters of each leachate were stored frozen for analyses, while the other 10 mL were temporarily stored in refrigerator before percolated through corresponding deep soils. In Stage 1, 11 leachates were collected for each surface soil sample,

2. Material and Methods

2.1. Sample Location and Preparation

Two landscape replicate soil cores E1 and E2 were collected to $\sim 1 \text{ m}$ depth in March 2015 from a site located in the Eight Mile Lake watershed of the Alaska Range ($\sim 670 \text{ m}$ elevation), Alaska, USA ($63^\circ 52' 59.64''\text{N}$, $149^\circ 13' 33.97''\text{W}$) (Figure 1) using a Snow, Ice, and Permafrost Research Establishment-style handheld drilling device. The site is located near the headwaters of a tributary (Tanana River) in the Yukon River drainage basin, on a well-drained gentle northeast facing slope (4%) [Natali *et al.*,

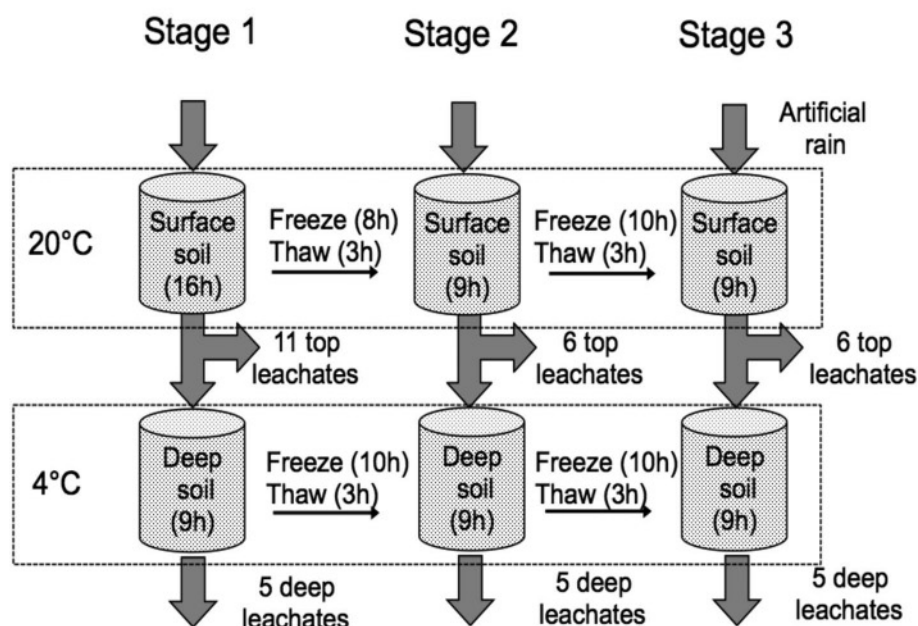


Figure 3. Leaching experimental procedure used in this experiment. Ten milliliters of each top leachate was used to leach deep soil. In stage 1, only top leachates from first, third, fifth, seventh, ninth, and eleventh collections were used. Due to absorption of water in the deep soils, only five deep leachates were collected in stage 1. For consistency, five deep leachates were collected in stages 2 and 3. Volumetric calculations were done on the input of top leachates to deep soils.

while 6 surface leachates were collected in Stages 2 and 3 using the same method. In Stage 1, every other 10 mL of surface leachate, starting from the first collection (total of 6), was used to sequentially leach deep soils. In Stages 2 and 3, 10 mL surface leachates from all collections were used to leach deep soil sequentially. Deep soil samples were leached in a 4°C cold room in darkness at the same rate as leaching upper soils. Samples used for FT-ICR-MS analysis were the first collected leachates in Stage 1 and combined leachates in Stage 3, based on the sample size requirement of OC.

The difference of results in surface and deep leachates were calculated as

$$\Delta X = X_D - X_S \quad (1)$$

where X_D is the amount of X (a parameter) in deep soil leachate (output) and X_S is the amount of X in surface soil leachate (input); a negative ΔX indicates retention, and a positive ΔX means releasing of materials from deep soils.

2.3. Total Organic Carbon, Total Nitrogen, and Dissolved Organic Carbon

Total organic carbon (TOC) and total nitrogen (TN) of soil samples were analyzed in the Light Stable Isotope Mass Spectrometry Lab at the University of Florida. Freeze-dried samples were decarbonated using HCl fumigation for 8 h [Harris *et al.*, 2001] and then dried at 60°C for 24 h. DOC concentrations of leachates were measured on a Shimadzu TOC-VCSN/TNM-1, using high-temperature catalytic oxidation [Guo *et al.*, 1994]. DOC concentrations were calculated from three to five injections, and the coefficient of variance was less than 2%.

2.4. UV-Vis Absorption and Fluorescence EEMs

UV-vis absorbance of leachates was measured between 200 nm and 600 nm on a Shimadzu UV-1800 spectrophotometer with 1 nm increments. Specific UV absorbance at 254 nm ($SUVA_{254}$) was calculated by dividing UV absorbance at 254 nm by DOC concentrations, resulting in units of $m^2 g C^{-1}$ as an indication of the percentage DOM aromaticity [Traina *et al.*, 1990; Weishaar *et al.*, 2003]. The absorption coefficient at 350 nm (a_{350}) was calculated as follows:

$$a_{350} = 2.303 \times A_{350} / r \quad (2)$$

where A is the absorbance measured across the path length r in meters. a_{350} has been used as an indicator for dissolved lignin phenol and CDOM concentrations [Hernes and Benner, 2003]. Spectral slope ratio (S_R), the

ratio of spectral slope $S_{275-295}$ over $S_{350-400}$, was determined via linear regression from the natural logarithm of absorbance between 275 and 295 and 350 and 400 nm, respectively. S_R was used as an index for DOM molecular weight [Helms *et al.*, 2008].

EEMs were generated by scanning excitation spectra (220–450 nm) and emission spectra (280–600 nm) at 5 and 1 nm increments on a Hitachi F-7000 Fluorescence Spectrophotometer, respectively. Parallel-factor analysis (PARAFAC) allowed for the separation of EEMs spectra into distinct components and estimates of the relative intensity of each component [Stedmon *et al.*, 2003]. PARAFAC modeling was executed via drEEM toolbox for MATLAB [Murphy *et al.*, 2013], and five components were validated using split half analysis (Figures S1 and S2).

2.5. FT-ICR-MS Sample Preparation and Analysis

Leachates were acidified with 6 N HCl to pH ~2–3, concentrated on Agilent Bond Elute PPL cartridges (200 mg), rinsed with acidified Milli-Q water (pH = 2), and eluted with one cartridge volume of methanol. The eluate was blown down to ~1 mL with gentle flow of nitrogen gas. The extracted samples were then directly infused into a 12 Tesla Bruker Solarix FT-ICR-MS (Bruker Daltonics Inc, Billerica, MA, USA) with an electrospray ionization source and analyzed in negative ion mode. All samples were analyzed at a resolving power of 400,000 ($m/\Delta m$ 50% at m/z 400) with mass range of 114 to 1200 m/z . For each sample, 144 scans were collected.

Data analysis software (Bruker Daltonik version 4.2) was used to convert raw spectra to peak lists by applying Fourier transform mass spectrometry peak picker with signal-to-noise (S:N) threshold of 7 and absolute intensity threshold of 100 with the following requirement $C_{0-100}H_{0-200}O_{0-50}N_{0-10}S_{0-2}P_{0-2}$, $H/C < 2.2$, $O/C < 1.2$, and $N/C < 0.5$ [Koch and Dittmar, 2006]. The observed masses in each sample were internally calibrated using an organic matter homologous series. The mass measurement accuracy after internal calibration was <1 ppm. Subsequently, elemental formulas were assigned using in-house built software, following the Compound Identification Algorithm, described by Kujawinski and Behn [2006]. Chemical formulas were assigned based on the following criteria: $S/N > 7$, mass measurement error <0.5 ppm. In addition, formulas that generated noninteger double-bond equivalences (DBEs) were not considered [Koch and Dittmar, 2006]. Double-bond equivalence (DBE) is computed as follows, based on Dittmar and Koch [2006]:

$$DBE = 1 + 0.5(2C - H + N + P) \quad (3)$$

Hydrophobicity, molecular weight distribution, and compound classes of samples were used to examine changes in molecular composition. Hydrophobic compounds were defined as $NSO:C \leq 0.1$ (molecular mass > 850 amu), and moderately hydrophobic compounds were defined as $0.1 < NSO:C < 0.49$ (molecular mass < 850 amu); hydrophilic compounds were defined as $NSO:C \geq 0.49$ (molecular mass < 850 amu); where $NSO:C$ is the ratio of number of nitrogen, sulfur, and oxygen atoms over number of carbon atoms in a compound [Liu and Kujawinski, 2015]. FT-ICR-MS formulas were assigned to the following compound classes: lipids, proteins, carbohydrates, amino sugars, lignin, tannins, and condensed hydrocarbons, based on elemental ratios of H:C and O:C [Minor *et al.*, 2014] (Figure S3a). Formulas with $DBE:C = 0.3–0.68$, $DBE:H = 0.2–0.95$, and $DBE:O = 0.77–1.75$ were assigned to be carboxylic-rich alicyclic molecules (CRAMs) [Hertkorn *et al.*, 2006]. The relative abundance of different compound classes was assessed using peak count and intensity-weighted percentage, which are the ratio of summed number and intensity of formulas in each class over the summed number and intensity of all formulas [Sleighter and Hatcher, 2008].

3. Results and Discussion

3.1. Bulk Mobilization of DOC

Cumulative DOC leached by artificial rain, percolated through pure organic surface soils (>40% TOC), approached asymptotic levels during the Stage 2, and remained stable until the end of Stage 3 (Figures 4a and 4b). Leaching removed 3.7 to 6.5% of OC in surface soil as DOC during the experiment (Table S1), which is higher than the soil DOC yield reported from other high-latitude tundra soils in short-term and long-term leaching experiments [Neff and Hooper, 2002; Guo *et al.*, 2007]. To confirm surface soil variability, we leached the surface sample (10–20 cm) from a third landscape replicate core, leading to 5.2% flux of soil OC (detailed data not shown here). Leaching of deep soils of this core was not possible because of their low permeability. For perspective, our field site receives an average of 245 mm of precipitation during the growing season

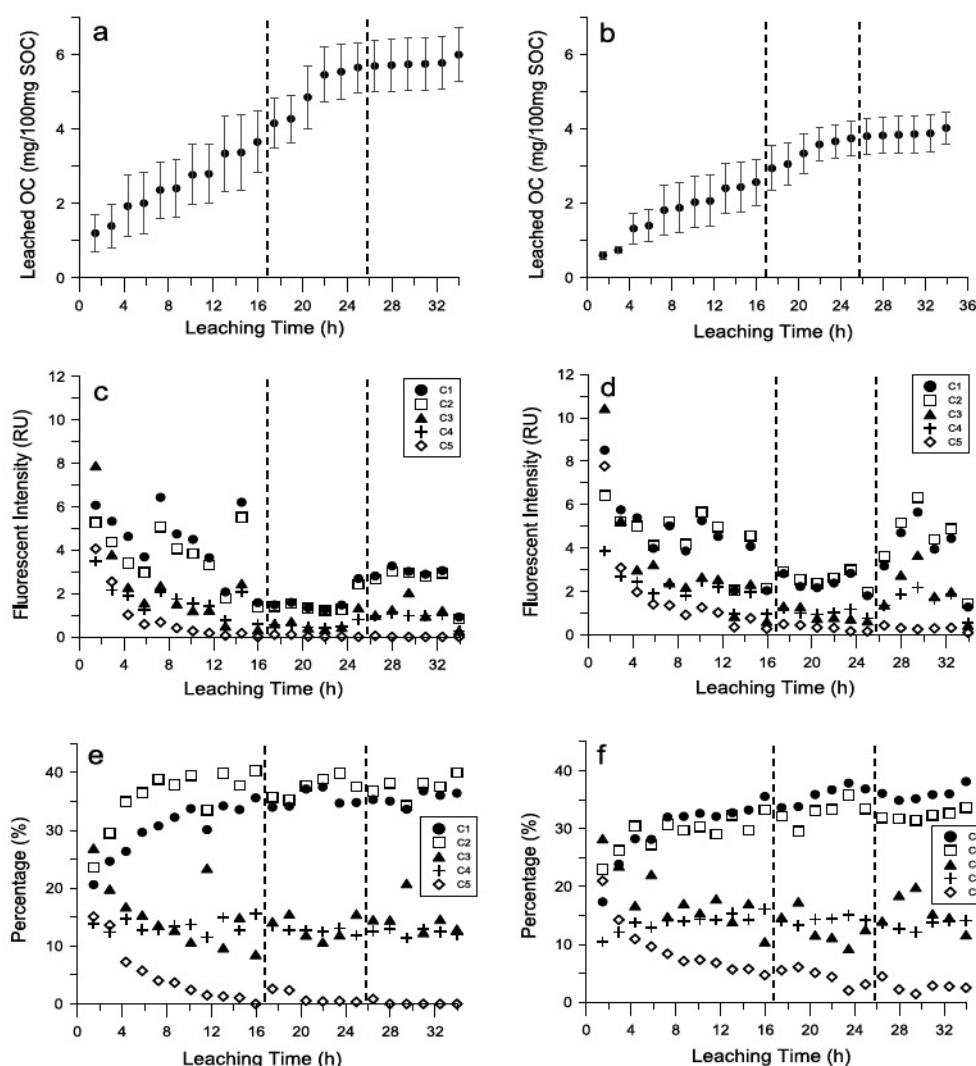


Figure 4. (a) Cumulative OC, (c) average fluorescent intensity, and (e) relative abundance of each component in surface soils from core E1. SOC in cumulative OC units means soil organic carbon. Relative abundance of five components was calculated by fluorescent intensity of each component divided by total fluorescent intensity. (b) Cumulative OC, (d) average fluorescent intensity, and (f) relative abundance of each component in surface soils from core E2. Dash lines indicate freezing overnight.

which is equal to 121 mL of leachate in our experiment. After 121 mL of leaching, 1.4%–3.0% of soil organic carbon (SOC) was leached from surface soils. In comparison, organic permafrost soils from around the Arctic respired an average of 6% OC when incubated in the laboratory at 5°C for 1 year [Trucco *et al.*, 2012; Schädel *et al.*, 2014]. While this value is difficult to compare to incubated soil losses, the relative magnitudes highlight the importance of quantifying lateral fluxes, in addition to heterotrophic respiration, when considering the C balance of Arctic ecosystems—especially at smaller scales (e.g., observational plots or local watersheds). Moreover, the effects of plant productivity and soil heterotrophs may enable more sustained DOC releases in field conditions compared to the asymptotic decrease in flux observed here. Finally, we note that despite temporal and spatial heterogeneity, the average water table depth for these soils is below the soil surface [Schädel *et al.*, 2016], so we can safely assume that the majority of precipitation flows either vertically (i.e., infiltration) or laterally (i.e., runoff) through surface soils.

The negative Δ OC in the first two stages indicated retention of DOC coming from surface soils (Figures 5a and 5b). At the beginning of Stage 3, deep soils appeared to be saturated as bulk DOC outputs matched inputs. At the end of the experiment, the total retention of OC from surface leachates by deep soils ranged from 2.4 to 3.2%

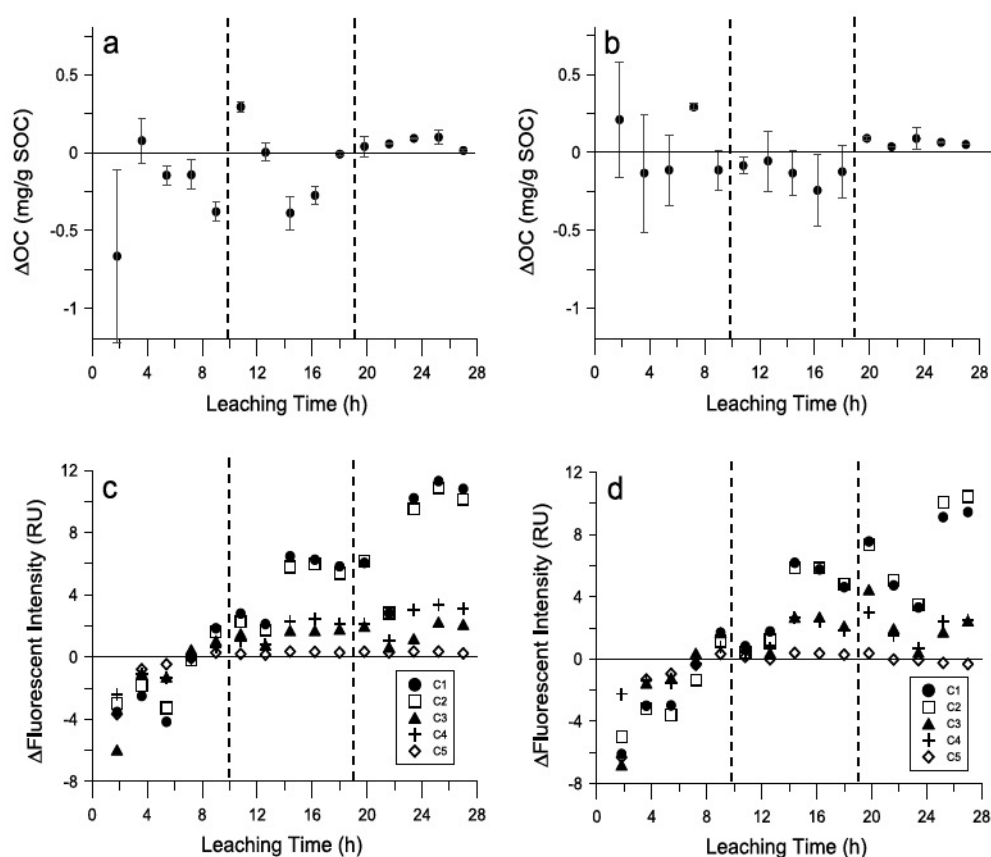


Figure 5. Δ OC in deep soils from cores (a) E1 and (b) E2. SOC in the unit means soil organic carbon. Δ fluorescent intensity of each component in deep soils from cores (c) E1 and (d) E2. Dash lines indicate freezing overnight.

in the pure organic deep soil (E2; ~44% TOC), and 19.0 to 27.3% in the organic-rich soil (E1; ~25% TOC, Table S2). The observed saturation during Stage 3 may also be a result of the low DOC inputs at that time, suggesting that the retentive capacity of deeper soils may be higher than observed here. Interestingly, these results suggest that retention of DOC in deep organic soils will likely increase with the deepening of the active layer, exposing more organic soils to thaw—at least on short timescales observed here. This clearly impacts the fate of DOC transported to streams/rivers in the Arctic [Spencer *et al.*, 2015]. To our knowledge, this is the first evidence for DOC retention in the organic soil column in Arctic soils, which is key to understand the behavior of DOC in different soil layers. Furthermore, these preliminary findings provide a mechanistic framework for predicting and understanding DOC export in different seasons, since thaw depth and precipitation varies throughout the year.

3.2. Spectrofluorometric Signatures of Soil DOM

SUVA₂₅₄, an indicator of DOM aromaticity, had values ($0.9 \pm 0.8 \text{ m}^2 \text{ g}^{-1} \text{ C}^{-1}$) in surface soils much lower than most Arctic river waters which is normally above $2 \text{ m}^2 \text{ g}^{-1} \text{ C}^{-1}$ [Spencer *et al.*, 2008; Stedmon *et al.*, 2011; Mann *et al.*, 2012; Wickland *et al.*, 2012; Mann *et al.*, 2016], indicating the abundance of nonchromophoric DOM in fresh and early-decomposed plant leachate (Figure 6a). Even though SUVA₂₅₄ was variable in surface soil leachates, a_{350} decreased with leaching time and reached an asymptotic state in Stage 2—similar to cumulative DOC (Figure 6c). The value of a_{350} at the beginning of leaching experiment was an order of magnitude higher than what commonly found in Arctic river DOM [Walker *et al.*, 2013] and decreased to riverine DOM values in Stage 3, reflective of the high amounts of aromatic compounds found in fresh and early-decomposed plant leachates. This also agrees with the relatively high a_{350} observed during spring freshet, when surface runoff only reacts with surface soils [Mann *et al.*, 2016].

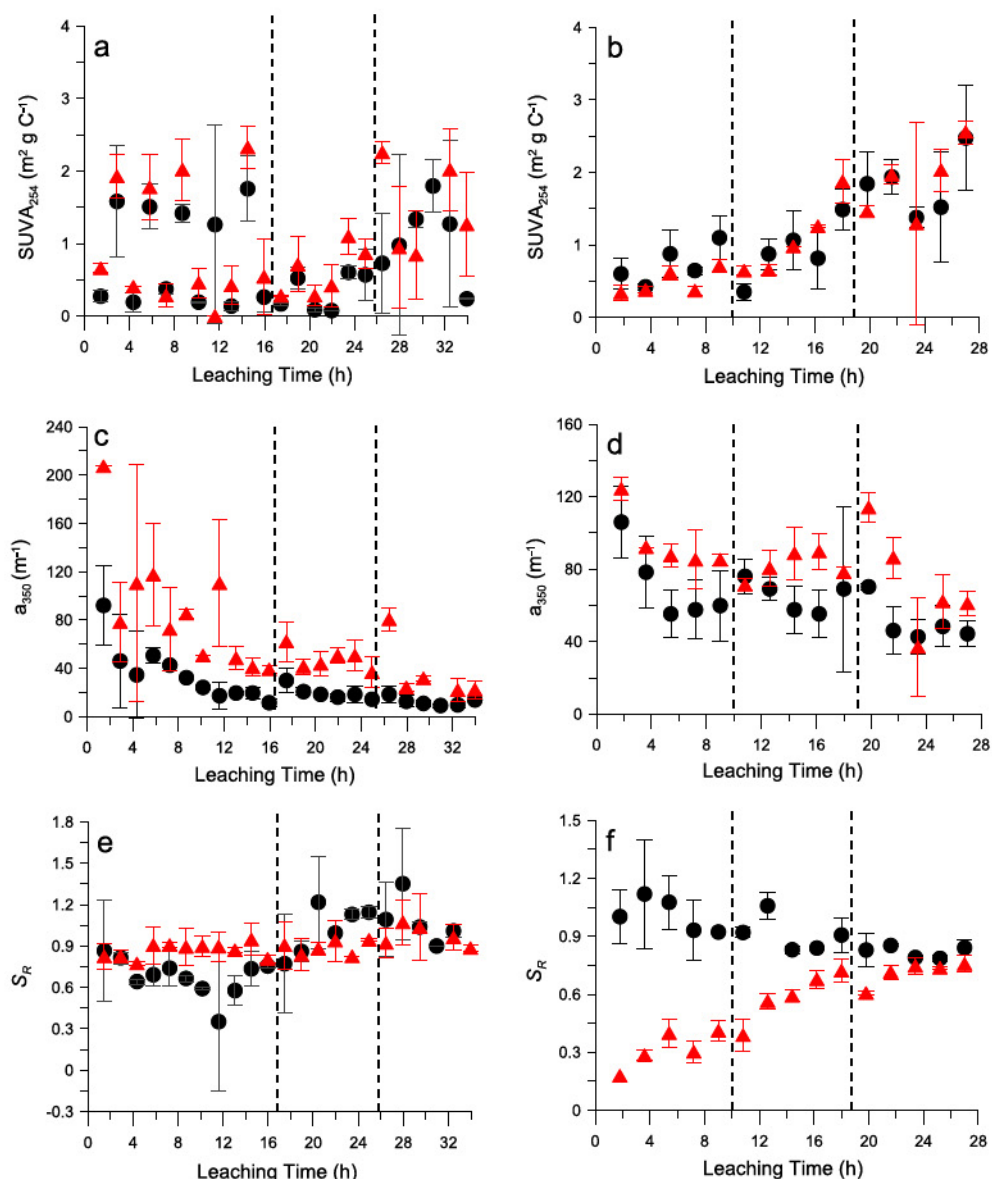


Figure 6. Scatter plots of (a) $SUVA_{254}$, (c) a_{350} , and (e) S_R from surface soils in cores E1 (black) and E2 (red). Scatterplots of (b) $SUVA_{254}$, (d) a_{350} , and (f) S_R from deep soils in cores E1 (black) and E2 (red). Dash lines indicate freezing overnight.

In deep soils, $SUVA_{254}$ increased with leaching time in both cores E1 ($r^2=0.7$, $p < 0.05$) and E2 ($r^2=0.8$, $p < 0.05$) (Figures 6b, S4a, and S4b) when the input of surface leachate had stable $SUVA_{254}$ values, indicating preferential leaching of CDOM. Recent work has shown a robust relationship between broad-scale CDOM and DOC comparisons in Arctic rivers, sampled at similar times with comparable procedures (e.g., the Arctic Great Rivers Observatory) [Mann *et al.*, 2016]. However, independent studies within a particular river basin (with more extensive sampling) have shown many cases with no significant relationship between CDOM and DOC, reflective of variable inputs of nonchromophoric DOM across Arctic watersheds [Mann *et al.*, 2016]. This discrepancy between CDOM and bulk DOC may be related to the selective transport of DOM (preferential leaching of CDOM) observed here, and may be variable due to site- and season-specific differences in hydrologic flow paths through watershed soils.

The CDOM-based index for molecular weight (S_R), showed increasing trends in surface leachate across Stages 1 and 3 in cores E1 and E2 (Figure 6e), indicating shifts from higher molecular weight (HMW) to lower molecular weight (LMW) CDOM. Interestingly, this shift to LMW with leaching time in surface soils corresponds

with Arctic river water molecular weight distributions during the spring freshet [Spencer *et al.*, 2009; Mann *et al.*, 2012], when most hydroflow only percolates through surface soils. More specifically, the increase of S_R during freshet from 0.8 to 1.0 [Mann *et al.*, 2012] agree with the increase of S_R in our leaching experiment at surface soils from 0.7 to 1.1 at E1 and 0.9 to 1.0 at E2 across Stages 1 and 3.

Deep-soil leachates from the two cores exhibited clearly opposite S_R trends, with E1 decreasing over time and E2 increasing (Figures 6f, S4e, and S4f). However, these trends converged toward the same S_R value by the end of leaching and, given that surface S_R values (i.e., inputs) were similar, suggested the presence of a LMW pool of CDOM in E1 that was removed during the experiment. The low value of S_R in E2 (pure organic, ~44% TOC) at the beginning of leaching experiment was consistent with the high abundance of HMW polymers in the initially degraded organic debris. Moreover, the fact that the deep cores started at very different S_R values and converged toward the end of the experiment suggests that similar leaching processes were likely operating in both cores.

PARAFAC modeling of EEMs spectrum yielded five components (Figure S1 and Table S3) that resembled literature spectra of humic, fulvic, and amino acids, etc. However, the potentially dubious nature of “geopolymers” [Schmidt *et al.*, 2011; Lehmann and Kleber, 2015], young age of these surficial organic soils [Hicks Pries *et al.*, 2013], and slowed processing of OC during cold winter temperatures lead us to conclude that the observed components are likely compounds released from the early decomposition of plant tissues (e.g., lignin, tannin, and proteins). Although there were distinct changes in relative intensity of different components over time (Figures 4e and 4f), their unequivocal identification caused us to use a pooled fluorescence intensity as our primary FDOM metric.

The net retention of bulk DOC in deep soils corresponded to a net FDOM release of $107.2 \pm 17.0\%$ and $52.9 \pm 1.7\%$ in cores E1 and E2, respectively (Figures 5a and 5b and Table S4). Bulk DOC showed variable retention and release during Stages 1 and 2 but remained stable during Stage 3, while net FDOM showed retention during Stage 1 and release during Stages 2 and 3 (Figures 5c and 5d). Stage 1 unambiguously retained both bulk DOC and FDOM indicating an abundance of reactive sites that allowed for adsorption. We interpret Stage 2 to be approaching a short-term equilibrium where selective retention and release began to occur as the reactive surface sites in the deep-soil approached saturation, consistent with the then-continuous release of FDOM and the variable retention of bulk DOC. By Stage 3, an apparent bulk DOC equilibrium was reached, with concurrent increases in the release of FDOM, indicating exchange on reactive surfaces resulting in the selective release of FDOM—consistent with the increase of $SUVA_{254}$ in deep soils. We contend that this large increase in fluorescent intensity during Stage 3 from surface to deep leachates ($81.0 \pm 10.2\%$), along with an equilibrium in bulk DOC, strongly indicates that nonfluorescent DOM must have been retained. This effect is especially relevant as the composition of exported DOM affects its apparent reactivity in streams and rivers [Vonk *et al.*, 2013b; Mann *et al.*, 2014]. In addition, the underlying process may help to explain why relict permafrost soils (i.e., yedoma) are depleted of phenolics [Spencer *et al.*, 2015], which we observed to trend toward preferential release with leaching. Additionally, the composition of leachates in our study did not appear to be impacted by overnight freezing, based on DOC, $SUVA_{254}$, and FDOM data in surface soils between leaching stages.

3.3. Molecular Character of DOM

Molecular data derived from FT-ICR-MS analyses were used to investigate the overall trends observed in bulk and spectroscopic data sets by leachate from Stages 1 and 3. In general, there were decreases in total peak counts ($58 \pm 13\%$) and assigned formulas ($59 \pm 13\%$), respectively (Table S5)—corresponding to a decrease in bulk DOC between two time points. However, peak counts and assigned formulas increased from surface to deep soils by 17.6% to 184.3% and 21.0% to 192.7% (Table S5), respectively, indicating that the deep soils exported a greater diversity of formulas. This was likely related to the depolymerization of plant tissues and transport of microbial biomass associated with degradation during the soil development [Lehmann and Kleber, 2015]. This increase in peak counts occurred even during Stage 3, when bulk DOC was at an apparent equilibrium, which further supports the notion that exchange was occurring between liquid (leachate) and solid (soil) phases, as documented earlier using our spectroscopic techniques. In general, the hydrophilic fraction of compounds decreased during leaching, with moderately hydrophobic fraction increasing in both surface and deep soils (Figures 7a and 7b), reflective of preferential leaching of hydrophilic compounds.

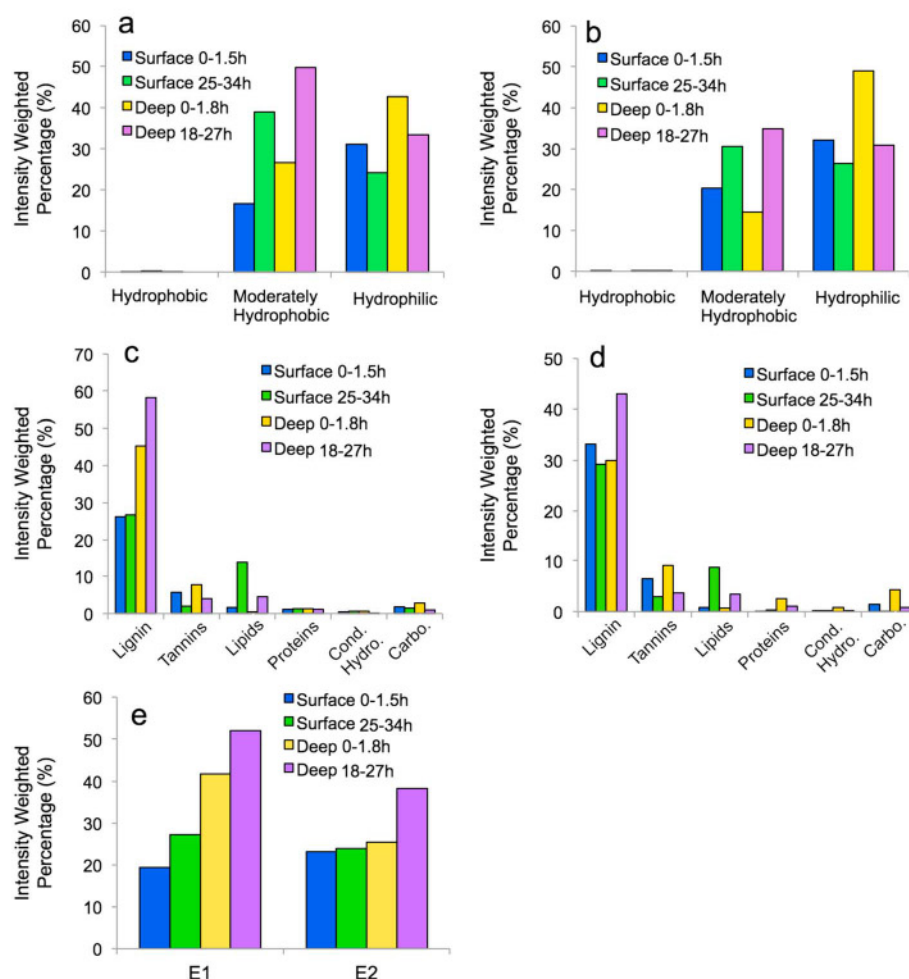


Figure 7. Intensity-weighted percentage of hydrophobic, moderately hydrophobic, and hydrophilic formulas in surface and deep leachates in core (a) E1 and (b) E2. Intensity-weighted percentage of different compound classes in surface and deep leachates in core (c) E1 and (d) E2. "Cond. Hydro." is short for "condensed hydrocarbon," while "Carbo." is short for "carbohydrates." (e) Intensity-weighted percentage of CRAM formulas for surface and deep samples in cores E1 and E2.

Molecular weight distributions of the leachate shifted to lower molecular weight (LMW) compounds (Figure S5) in surface soils by Stage 3, indicating preferential leaching of higher molecular weight (HMW) compounds during the experiment. It is also possible that the presence of some "humic" substances may have solubilized some of the hydrophobic HMW compounds, as humics have been known to enhance the solubility of hydrophobic substances in natural systems [Chiou *et al.*, 1987; Kim and Lee, 2002]. Hydrophobic substances can be incorporated into hydrophobic space of a large humic micelle [Wershaw, 1986; Von Wandruszka, 2000]. However, this did not agree with optical data likely due to difference in the target compound classes between those techniques. The reasons for the discrepancy include the following: (1) optical techniques only detect compounds which have chromophores or fluorophores (nonchromophoric DOM is not detectable), while mass spectroscopic can only analyze compounds which can be ionized [Oss *et al.*, 2010; Pereira *et al.*, 2014], and (2) selective loss of compounds during cartridge extraction for FT-ICR-MS analysis [Dittmar *et al.*, 2008; Chen *et al.*, 2016].

Compound classes were assigned based on elemental ratios of H:C and O:C [Minor *et al.*, 2014] (Figure S3a), of which lignin-like compounds were the major fraction (Figures 7c and 7d). These classifications are operationally defined and are ambiguous—as multiple chemical structures can have the same elemental formula. While all leachates were consistently dominated by lignin-like formulas, the percentage of lignin-like formulas in deep soils increased by 13.3% and 11.9% in peak count percentage and 13.1% and 13.0% in intensity-

weighted percentage from Stage 1 to Stage 3 (Figures 7c and 7d and Tables S5 and S6), respectively, which was consistent with CDOM and FDOM results of increasing aromatic contributions. This was also supported by an increase of the intensity-weighted percentage of lignin from surface leachate to deep soil leachates in Stage 3 in both cores E1 (by 118%) and E2 (by 47%) (Figures 7c and 7d and Table S6). The higher increase of lignin percentage in organic-rich soil (E1, ~25% TOC) than pure organic soils (E2, ~44% TOC) agreed with FI percentage change as discussed before, indicating enhanced fractionation by minerals. While lignin-like formulas increased through time, the percentage of tannin-like formulas decreased by 3.6% and 5.7%, while the percentage of protein-like formulas decreased by 0.1% and 1.5% in intensity-weighted percentage, respectively (Table S6). Tannin-like compounds, especially, resemble dissolved lignin using spectroscopic techniques. Thus, the significant and consistent decrease of tannin-like compounds likely corresponded to PARAFAC components that decreased through time (e.g., C4, C5, see Figures 4e and 4f), which supported observations reported for litter and soils [Hernes *et al.*, 2001]. However, our operational definitions of tannin- and lignin-like compounds most likely also include polyphenols released from *Sphagnum* moss litter [Verhoeven and Liefveld, 1997], which are abundant in our surface soils.

Carboxyl-rich alicyclic molecules (CRAMs) accounted for a substantial fraction of molecular formulas in soil leachates. The fraction of CRAM in peak count percentage were $51.0 \pm 7.1\%$ and $53.2 \pm 6.5\%$ in cores E1 and E2, respectively, while the fraction in intensity-weighted percentage were $35.1 \pm 14.7\%$ and $27.7 \pm 7.1\%$ in cores E1 and E2, respectively (Figure 7e and Tables S5 and S6). Interestingly, this supports recent work that showed CRAM as a major component of DOM collected from the Yukon River [Cao *et al.*, 2016]. The intensity-weighted percentage of CRAM increased with depth in the leaching experiment (Figure 7e), which autocorrelates with the increase of lignin and tannin compounds with depth—due to their large overlap in van Krevelen space [Stubbins *et al.*, 2010]. Despite representing a significant class of DOM compounds in aquatic systems [Leenheer, 1994; Hertkorn *et al.*, 2006], the biological origin of CRAM still remains poorly understood. Recent work in the Yukon River suggests that the CRAM in river DOM is largely derived from microbes [e.g., Amon *et al.*, 2012]. While we can only speculate at this time, the increase of CRAM from Stages 1 to 3, in both surface and deep soils, may reflect an increase in microbial activities with time of leaching.

The preferential leaching of aromatic components would likely result in higher amount of aromatic DOM in river water in summer than spring—when deep soils were thawed. However, other findings have shown that Arctic DOM in streams and rivers, during the spring freshet, tend to be enriched in aromatics and are young in age [Raymond *et al.*, 2007; Aiken *et al.*, 2014]. The seasonal pattern of riverine aromatic content is highly variable and suggests additional processes [Striegl *et al.*, 2007; Mann *et al.*, 2012]. This could be explained by long residence time and high temperature in the summer which enhance the microbial and photochemical decomposition of organic molecules [Striegl *et al.*, 2005; Wickland *et al.*, 2007].

3.4. Effect of Fractionation on Ecosystem Carbon Balance

The deep soils used in our experiment were located at the base of the contemporary active layer and are only exposed to hydroflow during the later growing season. As the active layer depth increases, deep soils will experience a greater portion of the seasonal hydroflow due to both thaw occurring earlier in the growing season as well as lengthening growing seasons with climate change [Barichivich *et al.*, 2013]. While the fate of leached OC in surface soil remains uncertain, we contend that a given parcel of surface leachate will be heavily altered during transport across the landscape. Our most quantitative representation of aromaticity, $SUVA_{254}$, is highly consistent with an initial increase in aromatic content during lateral transport and compares well with the higher values observed in Arctic rivers that have already passed through the landscape's soils [Mann *et al.*, 2012, 2014].

Fractionation of DOC by deep soils must, over time, influence the solid-phase composition of the deep soils as lignin and other aromatics are preferentially leached and other compounds are left behind. In addition, the retention of a portion of DOC, in either the solid-phase or the pore waters of deep soils, may also result in the accumulation of OC in deep soils. This vertical dissolved-phase OC translocation is consistent with observations of OC-enriched deep soils throughout high-latitude permafrost and supports other evidence for this phenomenon—such as the physical translation of solid soils due to cryoturbation [Bockheim, 2007; Kaiser *et al.*, 2007; Xu *et al.*, 2009; Gentsch *et al.*, 2015]. Sustained preferential leaching of aromatic contents may also, in part, explain for the aromatic-poor and aliphatic-enriched composition of leachates derived from yedoma

soils [Vonk et al., 2013a; Mann et al., 2015; Spencer et al., 2015]. The molecular character of retained DOM, which we only begin to infer, will be important to explore as the translocation of surface leachates may “prime” subsurface heterotrophic activity and result in enhanced soil degradation [Fontaine et al., 2004; Hartley et al., 2010].

4. Conclusion and Possible Implications

Our leaching experiment highlighted the potential release of DOM from surface soils, net retention of bulk surface soil DOM by deep soils, and indicated fractionation of compounds in soil leachate. We observed preferential leaching of aromatic compounds (e.g., lignin) and retention of nonchromophoric compounds from deep organic soils. This work highlights the importance of lateral flux of soil OC, due to leaching, when considering ecosystem carbon balances. Despite the difference in initial OC composition, similar processes were apparently operating in organic-rich and pure organic soils resulting in comparable FT-ICR-MS molecular weight and compound-class distributions and optical EEM, SUVA₂₅₄, and *S_R* indices. This fractionation of compounds during leaching may in part explain the composition of yedoma soils, which have undergone subsequent leaching, characterized by a depletion of aromatics and enrichment of aliphatics. These compounds, which are largely nonchromophoric, are important sources of DOC in streams/rivers in a thawing Arctic. This work also suggests the potential role of leachate export as an important mechanism of C losses from Arctic soils, in comparison the more traditional pathway from soil to atmosphere in a warming Arctic.

Future research is needed to understand the fate of leached surface DOM during lateral transport to streams and rivers as well as the portion retained by deep soils. The total retentive capacity of deep active layer soils is only hinted at with our results, and further, the integration of a watershed’s active layer soils presents compelling mass balance questions when considering landscape-scale lateral DOM fluxes. Deep organic soils have the potential to act as chromatographic media that selectively retain and release components of DOM, but this behavior on the watershed level as well as in soils of varying parent material is almost certainly highly variable. In addition, surface leachate DOM retained in the solid-phase is subject to in situ degradation by soil heterotrophs and, as such, these translocations may not result in the sequestration of surface DOM, especially in a warming climate. Improving our understanding of watershed-level chromatography is of utmost importance for interpreting DOM signatures observed in Arctic rivers and coasts.

Acknowledgments

Special thanks to Alexander L. Kholodov and Justin Ledman for their assistance during the sampling trip. FT-ICR-MS analysis was done at the Environmental Molecular Sciences Laboratory, a DOE user facility at Pacific Northwest National Laboratory. All other analyses were funded by the Jon and Beverly Thompson Chair in the department of Geological Sciences at University of Florida. The data used in the manuscript are available from the corresponding author (xz510@ufl.edu) and PANGAEA Data Archiving and Publication, and supporting data are included as six tables in a supporting information file.

References

- Aiken, G. R., R. G. M. Spencer, R. G. Striegl, P. F. Schuster, and P. A. Raymond (2014), Influences of glacier melt and permafrost thaw on the age of dissolved organic carbon in the Yukon River basin, *Global Biogeochem. Cycles*, 28, 525–537, doi:10.1002/2013GB004764.
- Amon, R. M. W., A. J. Rinehart, S. Duan, P. Louchouart, A. Prokushkin, G. Guggenberger, D. Bauch, C. Stedmon, P. A. Raymond, and R. M. Holmes (2012), Dissolved organic matter sources in large Arctic rivers, *Geochim. Cosmochim. Acta*, 94, 217–237.
- Barichivich, J., K. R. Briffa, R. B. Myneni, T. J. Osborn, T. M. Melvin, P. Ciais, S. Piao, and C. Tucker (2013), Large-scale variations in the vegetation growing season and annual cycle of atmospheric CO₂ at high northern latitudes from 1950 to 2011, *Global Change Biol.*, 19(10), 3167–3183.
- Bockheim, J. G. (2007), Importance of cryoturbation in redistributing organic carbon in permafrost-affected soils, *Soil Sci. Soc. Am. J.*, 71(4), 1335–1342.
- Bohan, L., H. M. Seip, and T. Larssen (1997), Response of two Chinese forest soils to acidic inputs: Leaching experiment, *Geoderma*, 75(1–2), 53–73.
- Cao, X., G. R. Aiken, R. G. M. Spencer, K. Butler, J. Mao, and K. Schmidt-Rohr (2016), Novel insights from NMR spectroscopy into seasonal changes in the composition of dissolved organic matter exported to the Bering Sea by the Yukon River, *Geochim. Cosmochim. Acta*, 181, 72–88.
- Chen, M., and R. Jaffé (2014), Photo- and bio-reactivity patterns of dissolved organic matter from biomass and soil leachates and surface waters in a subtropical wetland, *Water Res.*, 61, 181–190.
- Chen, M., S. Kim, J. E. Park, H. J. Jung, and J. Hur (2016), Structural and compositional changes of dissolved organic matter upon solid-phase extraction tracked by multiple analytical tools, *Anal. Bioanal. Chem.*, 408(23), 6249–6258.
- Chiou, C. T., D. E. Kile, T. I. Brinton, R. L. Malcolm, J. A. Leenheer, and P. MacCarthy (1987), A comparison of water solubility enhancements of organic solutes by aquatic humic materials and commercial humic acids, *Environ. Sci. Technol.*, 21(12), 1231–1234.
- Coble, P. G. (1996), Characterization of marine and terrestrial DOM in seawater using excitation-emission matrix spectroscopy, *Mar. Chem.*, 51(4), 325–346.
- Dittmar, T., and G. Kattner (2003), The biogeochemistry of the river and shelf ecosystem of the Arctic Ocean: A review, *Mar. Chem.*, 83(3), 103–120.
- Dittmar, T., and B. P. Koch (2006), Thermogenic organic matter dissolved in the abyssal ocean, *Mar. Chem.*, 102(3), 208–217.
- Dittmar, T., B. Koch, N. Hertkorn, and G. Kattner (2008), A simple and efficient method for the solid-phase extraction of dissolved organic matter (SPE-DOM) from seawater, *Limnol. Oceanogr. Methods*, 6(6), 230–235.
- Fontaine, S., G. Bardoux, L. Abbadie, and A. Mariotti (2004), Carbon input to soil may decrease soil carbon content, *Ecol. Lett.*, 7(4), 314–320.
- Frey, K. E., and J. W. McClelland (2009), Impacts of permafrost degradation on arctic river biogeochemistry, *Hydrol. Processes*, 23(1), 169–182.

- Gentsch, N., et al. (2015), Storage and transformation of organic matter fractions in cryoturbated permafrost soils across the Siberian Arctic, *Biogeosciences*, 12(14), 4525–4542.
- Guéguen, C., L. Guo, D. Wang, N. Tanaka, and C. C. Hung (2006), Chemical characteristics and origin of dissolved organic matter in the Yukon River, *Biogeochemistry*, 77(2), 139–155.
- Guo, L., and R. W. Macdonald (2006), Source and transport of terrigenous organic matter in the upper Yukon River: Evidence from isotope ($\delta^{13}\text{C}$, $\Delta^{14}\text{C}$, and $\delta^{15}\text{N}$) composition of dissolved, colloidal, and particulate phases, *Global Biogeochem. Cycles*, 20, GB2011, doi:10.1029/2005GB002593.
- Guo, L., C. H. Coleman, and P. H. Santschi (1994), The distribution of colloidal and dissolved organic carbon in the Gulf of Mexico, *Mar. Chem.*, 45(1), 105–119.
- Guo, L., C. L. Ping, and R. W. Macdonald (2007), Mobilization pathways of organic carbon from permafrost to arctic rivers in a changing climate, *Geophys. Res. Lett.*, 34, L13603, doi:10.1029/2007GL029582.
- Harris, D., W. R. Horváth, and C. van Kessel (2001), Acid fumigation of soils to remove carbonates prior to total organic carbon or carbon-13 isotopic analysis, *Soil Sci. Soc. Am. J.*, 65(6), 1853–1856.
- Hartley, I. P., D. W. Hopkins, M. Sommerkorn, and P. A. Wookey (2010), The response of organic matter mineralisation to nutrient and substrate additions in sub-arctic soils, *Soil Biol. Biochem.*, 42(1), 92–100.
- Helms, J. R., A. Stubbins, J. D. Ritchie, E. C. Minor, D. J. Kieber, and K. Mopper (2008), Absorption spectral slopes and slope ratios as indicators of molecular weight, source, and photobleaching of chromophoric dissolved organic matter, *Limnol. Oceanogr.*, 53(3), 955–969.
- Hemes, P. J., and R. Benner (2003), Photochemical and microbial degradation of dissolved lignin phenols: Implications for the fate of terrigenous dissolved organic matter in marine environments, *J. Geophys. Res.*, 108(C9), 3291, doi:10.1029/2002JC001421.
- Hemes, P. J., R. Benner, G. L. Cowie, M. A. Goñi, B. A. Bergamaschi, and J. I. Hedges (2001), Tannin diagenesis in mangrove leaves from a tropical estuary: A novel molecular approach, *Geochim. Cosmochim. Acta*, 65(18), 3109–3122.
- Hertkorn, N., R. Benner, M. Frommberger, P. Schmitt-Kopplin, M. Witt, K. Kaiser, A. Kettrup, and J. I. Hedges (2006), Characterization of a major refractory component of marine dissolved organic matter, *Geochim. Cosmochim. Acta*, 70(12), 2990–3010.
- Hicks Pries, C. E., E. A. Schuur, and K. G. Crummer (2012), Holocene carbon stocks and carbon accumulation rates altered in soils undergoing permafrost thaw, *Ecosystems*, 15(1), 162–173.
- Hicks Pries, C. E., E. A. Schuur, and K. G. Crummer (2013), Thawing permafrost increases old soil and autotrophic respiration in tundra: Partitioning ecosystem respiration using $\delta^{13}\text{C}$ and $\Delta^{14}\text{C}$, *Global Change Biol.*, 19(2), 649–661.
- Hicks Pries, C. E., R. S. Logtestijn, E. A. Schuur, S. M. Natali, J. H. Cornelissen, R. Aerts, and E. Dorrepaal (2015), Decadal warming causes a consistent and persistent shift from heterotrophic to autotrophic respiration in contrasting permafrost ecosystems, *Global Change Biol.*, 21(12), 4508–4519.
- Hodson, M., and S. Langan (1999), A long-term soil leaching column experiment investigating the effect of variable sulphate loads on soil solution and soil drainage chemistry, *Environ. Pollut.*, 104(1), 11–19.
- Intergovernmental Panel on Climate Change (2013), *Climate Change 2013: The Physical Science Basis. Contribution of Working Group I to the Fifth Assessment Report of the Intergovernmental Panel on Climate Change*, edited by T. F. Stocker et al., 1535 pp., Cambridge Univ. Press, New York.
- Kaiser, C., H. Meyer, C. Biasi, O. Rusalimova, P. Barsukov, and A. Richter (2007), Conservation of soil organic matter through cryoturbation in arctic soils in Siberia, *J. Geophys. Res.*, 112, G02017, doi:10.1029/2006JG000258.
- Kaiser, K., and K. Kalbitz (2012), Cycling downwards—dissolved organic matter in soils, *Soil Biol. Biochem.*, 52, 29–32.
- Kellerman, A. M., D. N. Kothawala, T. Dittmar, and L. J. Tranvik (2015), Persistence of dissolved organic matter in lakes related to its molecular characteristics, *Nat. Geosci.*, 8(6), 454–457.
- Kim, Y., and D. Lee (2002), Solubility enhancement of PCDD/F in the presence of dissolved humic matter, *J. Hazard. Mater.*, 91(1), 113–127.
- Koch, B. P., and T. Dittmar (2006), From mass to structure: An aromaticity index for high-resolution mass data of natural organic matter, *Rapid Commun. Mass Spectrom.*, 20(5), 926–932.
- Kujawinski, E. B., and M. D. Behn (2006), Automated analysis of electrospray ionization Fourier transform ion cyclotron resonance mass spectra of natural organic matter, *Anal. Chem.*, 78(13), 4363–4373.
- Kujawinski, E. B., P. G. Hatcher, and M. A. Freitas (2002), High-resolution Fourier transform ion cyclotron resonance mass spectrometry of humic and fulvic acids: Improvements and comparisons, *Anal. Chem.*, 74(2), 413–419.
- Leenheer, J. A. (1994), Chemistry of dissolved organic matter in rivers, lakes, and reservoirs, in *Environmental Chemistry of Lakes and Reservoirs*, Adv. Chem. Ser., vol. 237, edited by L. Baker, pp. 195–221, Am. Chem. Soc., Washington, D. C.
- Lehmann, J., and M. Kleber (2015), The contentious nature of soil organic matter, *Nature*, 528(7580), 60–68.
- Liu, Y., and E. B. Kujawinski (2015), Chemical composition and potential environmental impacts of water-soluble polar crude oil components inferred from ESI FT-ICR MS, *PLoS One*, 10(9), e0136376.
- Mann, P. J., A. Davydova, N. Zimov, R. G. M. Spencer, S. Davydov, E. Bulygina, S. Zimov, and R. M. Holmes (2012), Controls on the composition and lability of dissolved organic matter in Siberia's Kolyma River basin, *J. Geophys. Res.*, 117, G01028, doi:10.1029/2011JG001798.
- Mann, P. J., W. V. Sobczak, M. M. LaRue, E. Bulygina, A. Davydova, J. E. Vonk, J. Schade, S. Davydov, N. Zimov, and R. M. Holmes (2014), Evidence for key enzymatic controls on metabolism of Arctic river organic matter, *Global Change Biol.*, 20(4), 1089–1100.
- Mann, P. J., T. I. Eglinton, C. P. McIntyre, N. Zimov, A. Davydova, J. E. Vonk, R. M. Holmes, and R. G. Spencer (2015), Utilization of ancient permafrost carbon in headwaters of Arctic fluvial networks, *Nat. Commun.*, 6, doi:10.1038/ncomms8856.
- Mann, P. J., R. G. M. Spencer, P. J. Hernes, J. Six, G. R. Aiken, S. E. Tank, J. W. McClelland, K. D. Butler, R. Y. Dyda, and R. M. Holmes (2016), Pan-Arctic trends in terrestrial dissolved organic matter from optical measurements, *Front. Earth Sci.*, 4, 25.
- Mikan, C. J., J. P. Schimel, and A. P. Doyle (2002), Temperature controls of microbial respiration in arctic tundra soils above and below freezing, *Soil Biol. Biochem.*, 34(11), 1785–1795.
- Minor, E. C., M. M. Swenson, B. M. Mattson, and A. R. Oyler (2014), Structural characterization of dissolved organic matter: A review of current techniques for isolation and analysis, *Environ. Sci.: Processes Impacts*, 16(9), 2064–2079.
- Murphy, K. R., C. A. Stedmon, D. Graeber, and R. Bro (2013), Fluorescence spectroscopy and multi-way techniques. PARAFAC, *Anal. Methods*, 5(23), 6557–6566.
- Natali, S. M., E. A. Schuur, E. E. Webb, C. E. H. Pries, and K. G. Crummer (2014), Permafrost degradation stimulates carbon loss from experimentally warmed tundra, *Ecology*, 95(3), 602–608.
- Neff, J. C., and D. U. Hooper (2002), Vegetation and climate controls on potential CO_2 , DOC and DON production in northern latitude soils, *Global Change Biol.*, 8(9), 872–884.
- Neff, J. C., J. C. Finlay, S. A. Zimov, S. P. Davydov, J. J. Carrasco, E. A. G. Schuur, and A. I. Davydova (2006), Seasonal changes in the age and structure of dissolved organic carbon in Siberian rivers and streams, *Geophys. Res. Lett.*, 33, L23401, doi:10.1029/2006GL028222.

- O'Donnell, J. A., G. R. Aiken, M. A. Walvoord, P. A. Raymond, K. D. Butler, M. M. Dornblaser, and K. Heckman (2014), Using dissolved organic matter age and composition to detect permafrost thaw in boreal watersheds of interior Alaska, *J. Geophys. Res. Biogeosci.*, **119**, 2155–2170, doi:10.1002/2014JG002695.
- Oss, M., A. Krueve, K. Herodes, and I. Leito (2010), Electrospray ionization efficiency scale of organic compounds, *Anal. Chem.*, **82**(7), 2865–2872.
- Osterkamp, T. E. (2007), Characteristics of the recent warming of permafrost in Alaska, *J. Geophys. Res.*, **112**, F02S02, doi:10.1029/2006JF000578.
- Pereira, R., C. Isabella Bovolo, R. G. M. Spencer, P. J. Hernes, E. Tipping, A. Vieth-Hillebrand, N. Pedentchouk, N. A. Chappell, G. Parkin, and T. Wagner (2014), Mobilization of optically invisible dissolved organic matter in response to rainstorm events in a tropical forest head-water river, *Geophys. Res. Lett.*, **41**, 1202–1208, doi:10.1002/2013GL058658.
- Raymond, P. A., J. W. McClelland, R. M. Holmes, A. V. Zhulidov, K. Mull, B. J. Peterson, R. G. Striegl, G. R. Aiken, and T. Y. Gurtovaya (2007), Flux and age of dissolved organic carbon exported to the Arctic Ocean: A carbon isotopic study of the five largest arctic rivers, *Global Biogeochem. Cycles*, **21**, GB4011, doi:10.1029/2007GB002934.
- Rowland, J. C., et al. (2010), Arctic landscapes in transition: Responses to thawing permafrost, *EOS Trans. AGU*, **91**(26), 229–236.
- Schädel, C., E. A. G. Schuur, R. Bracho, B. Elberling, C. Knoblauch, H. Lee, Y. Luo, G. R. Shaver, and M. R. Turetsky (2014), Circumpolar assessment of permafrost C quality and its vulnerability over time using long-term incubation data, *Global Change Biol.*, **20**(2), 641–652.
- Schädel, C., E. A. G. Schuur, M. Taylor, M. Mauritz, S. Natali, and J. Ledman (2016), Eight Mile Lake Research Watershed, Carbon in Permafrost Experimental Heating Research (GPEHR): Seasonal water table depth data, 2016, Bonanza Creek LTER - Univ. of Alaska Fairbanks. BNZ554, doi:10.6073/pasta/8547cd619095555620e7f3573435e72.
- Schmidt, M. W., M. S. Torn, S. Abiven, T. Dittmar, G. Guggenberger, I. A. Janssens, M. Kleber, I. Kögel-Knabner, J. Lehmann, and D. A. Manning (2011), Persistence of soil organic matter as an ecosystem property, *Nature*, **478**(7367), 49–56.
- Schuur, E. A. G., J. G. Vogel, K. G. Crummer, H. Lee, J. O. Sickman, and T. E. Osterkamp (2009), The effect of permafrost thaw on old carbon release and net carbon exchange from tundra, *Nature*, **459**(7246), 556–559.
- Schuur, E. A. G., A. D. McGuire, C. Schädel, G. Grosse, J. W. Harden, D. J. Hayes, G. Hugelius, C. D. Koven, P. Kuhry, and D. M. Lawrence (2015), Climate change and the permafrost carbon feedback, *Nature*, **520**(7546), 171–179.
- Sistla, S. A., J. C. Moore, R. T. Simpson, L. Gough, G. R. Shaver, and J. P. Schimel (2013), Long-term warming restructures Arctic tundra without changing net soil carbon storage, *Nature*, **497**(7451), 615–618.
- Sleighter, R. L., and P. G. Hatcher (2007), The application of electrospray ionization coupled to ultrahigh resolution mass spectrometry for the molecular characterization of natural organic matter, *J. Mass Spectrom.*, **42**(5), 559–574.
- Sleighter, R. L., and P. G. Hatcher (2008), Molecular characterization of dissolved organic matter (DOM) along a river to ocean transect of the lower Chesapeake Bay by ultrahigh resolution electrospray ionization Fourier transform ion cyclotron resonance mass spectrometry, *Mar. Chem.*, **110**(3), 140–152.
- Spencer, R. G., G. R. Aiken, K. P. Wickland, R. G. Striegl, and P. J. Hernes (2008), Seasonal and spatial variability in dissolved organic matter quantity and composition from the Yukon River basin, Alaska, *Global Biogeochem. Cycles*, **22**, GB4002, doi:10.1029/2008GB003231.
- Spencer, R. G., G. R. Aiken, K. D. Butler, M. M. Dornblaser, R. G. Striegl, and P. J. Hernes (2009), Utilizing chromophoric dissolved organic matter measurements to derive export and reactivity of dissolved organic carbon exported to the Arctic Ocean: A case study of the Yukon River, Alaska, *Geophys. Res. Lett.*, **36**, L06401, doi:10.1029/2008GL036831.
- Spencer, R. G., P. J. Mann, T. Dittmar, T. I. Eglinton, C. McIntyre, R. M. Holmes, N. Zimov, and A. Stubbins (2015), Detecting the signature of permafrost thaw in Arctic rivers, *Geophys. Res. Lett.*, **42**, 2830–2835, doi:10.1002/2015GL063498.
- Stedmon, C. A., S. Markager, and R. Bro (2003), Tracing dissolved organic matter in aquatic environments using a new approach to fluorescence spectroscopy, *Mar. Chem.*, **82**(3), 239–254.
- Stedmon, C. A., R. M. W. Amon, A. J. Rinehart, and S. A. Walker (2011), The supply and characteristics of colored dissolved organic matter (CDOM) in the Arctic Ocean: Pan Arctic trends and differences, *Mar. Chem.*, **124**(1), 108–118.
- Striegl, R. G., G. R. Aiken, M. M. Dornblaser, P. A. Raymond, and K. P. Wickland (2005), A decrease in discharge-normalized DOC export by the Yukon River during summer through autumn, *Geophys. Res. Lett.*, **32**, L21413, doi:10.1029/2005GL024413.
- Striegl, R. G., M. M. Dornblaser, G. R. Aiken, K. P. Wickland, and P. A. Raymond (2007), Carbon export and cycling by the Yukon, Tanana, and Porcupine rivers, Alaska, 2001–2005, *Water Resour. Res.*, **43**, W02411, doi:10.1029/2006WR005201.
- Stubbins, A., R. G. Spencer, H. Chen, P. G. Hatcher, K. Mopper, P. J. Hernes, V. L. Mwamba, A. M. Mangangu, J. N. Wabakanganzi, and J. Six (2010), Illuminated darkness: Molecular signatures of Congo River dissolved organic matter and its photochemical alteration as revealed by ultrahigh precision mass spectrometry, *Limnol. Oceanogr.*, **55**(4), 1467–1477.
- Tarnocai, C., J. G. Canadell, E. A. G. Schuur, P. Kuhry, G. Mazhitova, and S. Zimov (2009), Soil organic carbon pools in the northern circumpolar permafrost region, *Global Biogeochem. Cycles*, **23**, GB2023, doi:10.1029/2008GB003327.
- Traina, S. J., J. Novak, and N. E. Smeck (1990), An ultraviolet absorbance method of estimating the percent aromatic carbon content of humic acids, *J. Environ. Qual.*, **19**(1), 151–153.
- Trucco, C., E. A. G. Schuur, S. M. Natali, E. F. Belshe, R. Bracho, and J. Vogel (2012), Seven-year trends of CO₂ exchange in a tundra ecosystem affected by long-term permafrost thaw, *J. Geophys. Res.*, **117**, G02031, doi:10.1029/2011JG001907.
- Verhoeven, J. T. A., and W. M. Liefveld (1997), The ecological significance of organochemical compounds in Sphagnum, *Acta Bot. Neerl.*, **46**(2), 117–130.
- Von Wandruszka, R. (2000), Humic acids: Their detergent qualities and potential uses in pollution remediation, *Geochem. Trans.*, **1**(1), 1.
- Vonk, J. E., P. J. Mann, S. Davydov, A. Davydova, R. G. Spencer, J. Schade, W. V. Sobczak, N. Zimov, S. Zimov, and E. Bulygina (2013a), High biolability of ancient permafrost carbon upon thaw, *Geophys. Res. Lett.*, **40**, 2689–2693, doi:10.1002/grl.50348.
- Vonk, J. E., P. J. Mann, K. L. Dowdy, A. Davydova, S. P. Davydov, N. Zimov, R. G. M. Spencer, E. B. Bulygina, T. I. Eglinton, and R. M. Holmes (2013b), Dissolved organic carbon loss from Yedoma permafrost amplified by ice wedge thaw, *Environ. Res. Lett.*, **8**(3), 035023.
- Walker, S. A., R. M. Amon, and C. A. Stedmon (2013), Variations in high-latitude riverine fluorescent dissolved organic matter: A comparison of large Arctic rivers, *J. Geophys. Res. Biogeosci.*, **118**, 1689–1702, doi:10.1002/2013JG002320.
- Ward, C. P., and R. M. Cory (2015), Chemical composition of dissolved organic matter draining permafrost soils, *Geochim. Cosmochim. Acta*, **167**, 63–79.
- Weishaar, J. L., G. R. Aiken, B. A. Bergamaschi, M. S. Fram, R. Fujii, and K. Mopper (2003), Evaluation of specific ultraviolet absorbance as an indicator of the chemical composition and reactivity of dissolved organic carbon, *Environ. Sci. Technol.*, **37**(20), 4702–4708.
- Wershaw, R. L. (1986), A new model for humic materials and their interactions with hydrophobic organic chemicals in soil-water or sediment-water systems, *J. Contam. Hydrol.*, **1**(1–2), 29–45.

- Wickland, K. P., J. C. Neff, and G. R. Aiken (2007), Dissolved organic carbon in Alaskan boreal forest: Sources, chemical characteristics, and biodegradability, *Ecosystems*, *10*(8), 1323–1340.
- Wickland, K. P., G. R. Aiken, K. Butler, M. M. Dornblaser, R. G. M. Spencer, and R. G. Striegl (2012), Biodegradability of dissolved organic carbon in the Yukon River and its tributaries: Seasonality and importance of inorganic nitrogen, *Global Biogeochem. Cycles*, *26*, GB0E03, doi:10.1029/2012GB004342.
- Xu, C., L. Guo, C.-L. Ping, and D. M. White (2009), Chemical and isotopic characterization of size-fractionated organic matter from cryoturbated tundra soils, northern Alaska, *J. Geophys. Res.*, *114*, G03002, doi:10.1029/2008JG000846.